

Photocatalytic Activity of a Multicomponent System Assembled within Zeolites: Case of 2,4,6-Triphenylpyrylium or Ruthenium Tris(bipyridyl) Photosensitizers and Titanium Dioxide Relays within Zeolite Y

Gonzalo Cosa,[†] Michelle N. Chrétien,[†] María S. Galletero,[‡] Vicente Fornés,[‡] Hermenegildo García,^{*,‡} and J. C. Scaiano^{*,†}

Department of Chemistry, Center for Catalysis Research and Innovation, University of Ottawa, Ottawa K1N 6N5, Canada, and Instituto de Tecnología Química, CSIC-UPV, Universidad Politécnica de Valencia, Apartado 22012, 46071-Valencia, Spain

Received: June 6, 2001; In Final Form: October 8, 2001

Samples of zeolite Y containing 2,4,6-triphenylpyrylium or tris(bipyridyl)ruthenium(II) have been prepared and their photophysical and photochemical properties compared to those of the same samples containing encapsulated nanoscopic TiO₂ clusters as relays. The emission of encapsulated Ru(bpy)₃²⁺ and TP⁺ photolumophores undergoes static quenching in the presence of codoped TiO₂ clusters. This is the expected behavior for systems, where photosensitizer and relay lack diffusional mobility. Time-resolved diffuse reflectance laser flash photolysis shows the transient generation of TP[•] pyranil radical and Ru(bpy)₃³⁺, upon irradiation of TP⁺ and Ru(bpy)₃²⁺ in the presence of TiO₂, respectively. This provides firm support for the occurrence of photoinduced electron transfer between excited TP⁺ as acceptor and TiO₂ clusters as donors and from Ru(bpy)₃²⁺ to the conduction band of TiO₂. Using the photoinactivation of horseradish peroxidase as a test reaction in aqueous medium, a synergism has been found with respect to the activity of Ru(bpy)₃²⁺ or TP⁺ photocatalysts when incorporated inside the supercages of zeolite Y in the presence of TiO₂ nanoclusters.

Introduction

The nondeformable internal cavities defined by the rigid crystal structure of microporous zeolites provide a compartmentalized space for the design of multicomponent photochemical systems where each part is spatially arranged with respect to the other components.^{1–5} After the assembly at a molecular level of such a photochemical material, the system will remain ordered in a way reminiscent of the manner in which nature organizes photosynthetic centers. The role of the photochemically inert protein in natural systems would be played by the robust inorganic structure of the zeolite, embedding and holding in place each of the components. The similarity existing between systems based on zeolites and biologically active macromolecules has been noted in the past, and the term *zeozymes* has been coined.^{6–11} For instance, metal phthalocyanines have been obtained inside the cavities of zeolites X and Y and the resulting immobilized complex exhibits activity for the epoxidation of alkenes by hydroperoxides in a way that has some parallel to cytochrome P450. However, examples realizing and developing the potential of this methodology are still very scarce. In addition, the special properties of the medium defined by the zeolite internal voids can contribute to enhance the efficiency of certain photochemical reaction pathways.¹² For instance, the ability of zeolites to favor photoinduced electron-transfer reactions and to retard undesired back electron transfer is well documented.¹³

A major challenge in developing these systems consists of devising an efficient assembly procedure that ensures the correct

ordering of components. There are a large number of examples demonstrating that energy^{14–17} and electron-transfer photosensitization^{12,17,18} between adsorbed molecules within the zeolite cavities can occur efficiently without the need of covalent bonding between components. However, in the case of multicomponent photochemical systems it remains to be demonstrated that this can result in a synergistic effect when compared to the isolated components.

Some time ago, we reported the ship-in-a-bottle synthesis of 2,4,6-triphenylpyrylium ion (TP⁺) encapsulated inside the supercages of zeolite Y (TPY).¹⁸ After the synthesis, TP⁺ is too large to diffuse out of the cages and remains mechanically immobilized in the pores. However, TP⁺ is still able to interact with electron donor molecules provided they are sufficiently small for diffusion through the zeolite Y micropores.^{19,20} Previous studies from our groups have shown that encapsulation inside the zeolite modifies the molecular and photochemical properties of TP⁺. Particularly, TP⁺ immobilized inside zeolites Y and Beta is indefinitely persistent in aqueous suspensions at neutral pH and photolysis results in the generation of hydroxyl radicals.²⁰ This finding has triggered the use of TPY both as a *positive* (synthetic)²¹ and *negative* (degradative)^{20,22} photocatalytic system.

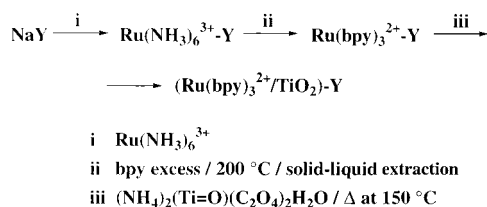
Several groups,^{23–33} including ours,^{34,35} have prepared nanoclusters of TiO₂ included in large and medium pore sized zeolites. The purpose of this research is to gain control over the photoactivity of TiO₂ by means of *quantum size effects* and shape selectivity. Until now, this type of research has been limited to time-resolved studies and a relatively small number of photocatalytic tests for NO_x decomposition and CO₂ reduction.^{26,27} Most of the potential of this methodology in tuning the activity of TiO₂ and developing new multicomponent

* Corresponding authors. E-mail (H.G.): hgarcia@qim.upv.es.

[†] University of Ottawa.

[‡] Universidad Politécnica de Valencia.

SCHEME 1



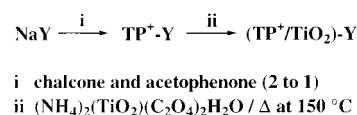
photoactive systems is still to be realized, and this work constitutes an effort in that direction.

We report here the assembly of two-component systems consisting of TiO_2 nanoclusters and an organic or organometallic photosensitizing dye, both contained within the voids of zeolite Y. As photosensitizers we selected two dyes of opposite behavior: tris(bipyridyl)ruthenium(II), which acts as an electron donor, and 2,4,6-triphenylpyrylium, which is a strong electron acceptor.^{36–49} The ability of electron donor dyes, particularly those derived from tris(bipyridyl)ruthenium(II) complex and phthalocyanines, to inject an electron into the TiO_2 semiconductor conduction band is very well-known and finds application in solar cells.^{46,50–60} The system of external $\text{Ru}(\text{bpy})_3^{2+}$ bound to colloidal TiO_2 , associated externally to zeolite L containing encapsulated $\text{MV}^{2+}\text{-Pt}$, constitutes a related precedent to our work.⁴ Less documented is the combination of TiO_2 with an electron-accepting photosensitizer, such as TP^+ . In its singlet or triplet excited state, TP^+ behaves as a powerful electron acceptor ($E_{\text{ox}} = 2.1$ V vs SCE)³⁶ able to abstract one electron from the semiconductor valence band of TiO_2 generating a positive hole (h^+). In this work we present evidence for the interaction between the electron donor $[\text{Ru}(\text{bpy})_3^{2+}]$ and acceptor (TP^+) photosensitizing dyes and TiO_2 clusters. These results have been obtained by steady-state and time-resolved emission and diffuse reflectance absorption spectroscopies. Interestingly, the interaction between TiO_2 and the photosensitizer leads to an enhancement in the photocatalytic activity of these two-component systems, with respect to samples containing only a single component, for the photochemical deactivation of horseradish peroxidase. During the preparation of this manuscript a report has come to our attention wherein a material containing coadsorbed $\text{Ru}(\text{bpy})_3^{2+}$ and TiO_2 in zeolite Y was prepared.⁶¹ Although the coincidence in the subject of both articles is marginal, since characterization techniques and reactions under investigation are different, the publication of a paper containing the preparation and photocatalytic properties of $\text{Ru}(\text{bpy})_3^{2+}\text{-TiO}_2$ in zeolite Y is evidence of the current interest in these types of materials.

Results and Discussion

Preparation of these two-component photocatalytic systems was accomplished by a stepwise procedure. Both TP^+ and $\text{Ru}(\text{bpy})_3^{2+}$ photosensitizers can be accommodated inside the large cavities of zeolite Y, but they are too big (~ 13 Å for both molecules) to diffuse through the smaller cavity windows (7.4 Å) and require preparation by ship-in-a-bottle synthesis from smaller precursors. After formation, these large photosensitizer molecules remain immobilized inside the cavities. TP^+ and $\text{Ru}(\text{bpy})_3^{2+}$ within zeolite Y were obtained according to previously reported procedures as indicated in Schemes 1 and 2, and their spectroscopic properties are in agreement with those in the literature.^{18,49,61} The photosensitizer content in the zeolites was determined by combustion chemical analyses of the organic material present in these crystal structures. The intracrystalline location of these dyes has been inferred from the failure to

SCHEME 2



recover these ions by solid–liquid extraction or ion exchange. The homogeneous distribution throughout the particles relies on the faster diffusion of precursors $[\text{Ru}(\text{NH}_3)_6^{3+}]$ and bpy compared to formation of the species and has yet been demonstrated. Encapsulation of the photosensitizer prior to the formation of TiO_2 clusters was preferred since we reasoned that the massive presence of TiO_2 blocking the pores would make synthesis of the photosensitizer within the cavities much more difficult.

Following the preparation of the photosensitizers inside the zeolite, the samples were submitted to ion exchange using aqueous solutions of the mixed titanylammmonium oxalate salt and mild calcination by baking the samples at 150 °C. This procedure has been shown to yield high loadings of TiO_2 clusters essentially leaving the zeolite with no free pore volume while the mild temperatures required are not high enough to produce any significant decomposition of the dyes. Independent thermogravimetric and spectroscopic studies have revealed that these dyes are completely stable below 300 °C. On the other hand, formation of TiO_2 nanoscopic clusters can be assessed from disappearance of the Ti=O^{2+} bands in Raman spectroscopy.^{23,24,62}

In a recent reference,⁶¹ TiO_2 was introduced to a similar sample via ion exchange with explosive TiCl_3 . This procedure was carried out under strict inert atmosphere in ethylene glycol followed by subsequent hydrolysis and air oxidation. Other related reports include the assembly of $\text{Ru}(\text{bpy})_3^{2+}\text{-colloidal TiO}_2$ particles adsorbed on the external surface of mordenite by Mallouk and co-workers.⁴

Spectroscopic characterization of the resulting two-component photocatalysts by UV and IR spectroscopy showed the features characteristic of TP^+ or $\text{Ru}(\text{bpy})_3^{2+}$ within zeolite Y, accompanied with some features corresponding to TiO_2 (see Figures 1 and 2). In the IR spectra, all of the peaks corresponding to $\text{Ru}(\text{bpy})_3^{2+}$ or TP^+ in the 1800–1300 cm^{-1} region are still present, together with a broad band at 1700 cm^{-1} introduced by TiO_2 . The presence of TiO_2 clusters is confirmed in the diffuse reflectance UV–vis spectra (DRS) of the solids by an increase of the absorption at about 250 nm that is not present in the absence of TiO_2 . An increased absorption throughout the 358–800 nm region was recently reported as a sign of the interaction between $\text{Ru}(\text{bpy})_3^{2+}$ and TiO_2 inside zeolite Y.⁶¹ Our samples do not exhibit a significant absorption in the long wavelength region as can be seen in Figure 2A. Table 1 summarizes the main analytical and spectroscopic properties of the samples whose photocatalytic activities have been tested.

TP^+ and $\text{Ru}(\text{bpy})_3^{2+}$ photosensitizers embedded within zeolite Y exhibit characteristic emission upon excitation in the corresponding absorption maxima.^{41,63,64} In the case of $\text{Ru}(\text{bpy})_3^{2+}$ encapsulated within zeolite Y, previous literature work has shown that the intensity and lifetime of this emission are influenced by the presence of quenchers. A case that has attracted considerable attention is the quenching of the excited state of $\text{Ru}(\text{bpy})_3^{2+}$ by methyl viologen.^{41,45} In our case, comparison of the steady-state emission of the original $\text{Ru}(\text{bpy})_3\text{Y}$ with that of the same solid also containing TiO_2 shows a ca. 25% decrease in the total emission intensity as measured by the area of the photoluminescence spectra (Figure

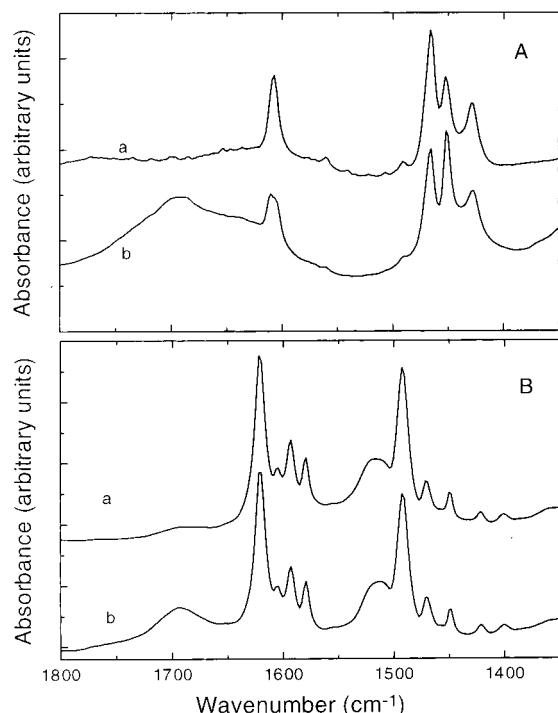


Figure 1. Aromatic region of the FT-IR spectra of $\text{Ru}(\text{bpy})_3^{2+}$ (A) and TP^+ (B) encapsulated within zeolite Y after outgassing at 200 °C under 10^{-2} Pa for 1 h, before (a) and after (b) inclusion of TiO_2 .

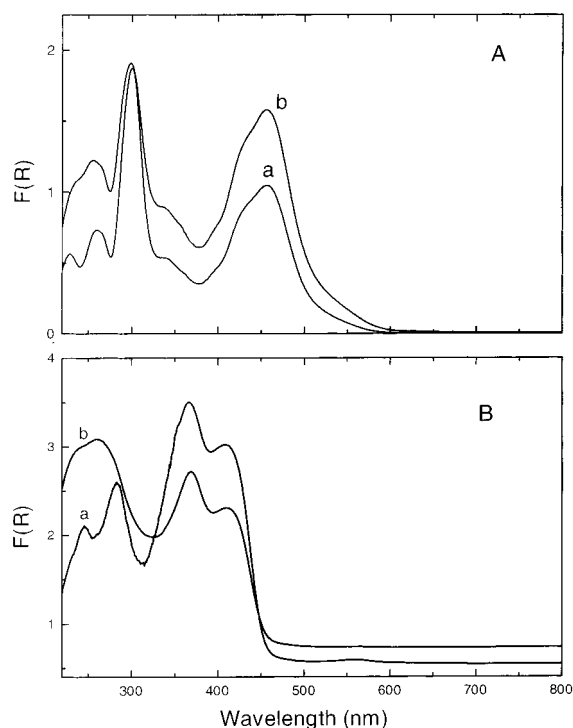


Figure 2. Diffuse reflectance spectra [plotted as the Kubelka–Munk function $F(R)$] of $\text{Ru}(\text{bpy})_3^{2+}$ (A) and TP^+ (B) before (a) and after (b) incorporation of TiO_2 .

3). In contrast, the reduction of the overall TP^+ photoluminescence is not as remarkable as the distinct change in shape (Figure 4). The emission of TPY consists of a superposition of fluorescence (λ_{fl} 470 nm) and phosphorescence (λ_{ph} 560 nm).⁶⁴ The variation in shape can be interpreted as indicating a significant quenching of the singlet excited state emission and an increase in phosphorescence from the triplet excited state. Considering only the emission from 430 to 540 nm, which

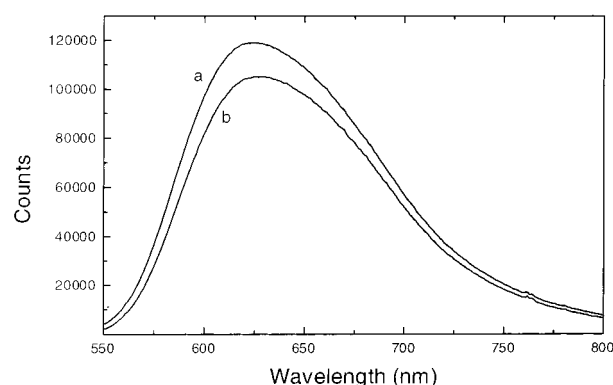


Figure 3. Emission spectra of the $\text{Ru}(\text{bpy})_3^{2+}\text{-Y}$ (a) and $(\text{Ru}(\text{bpy})_3^{2+}/\text{TiO}_2)\text{-Y}$ (b) samples upon 466 nm excitation. The total area of photoluminescence spectra was $(2.3 \pm 0.2) \times 10^7$ and $(1.7 \pm 0.1) \times 10^7$ for a and b, respectively.

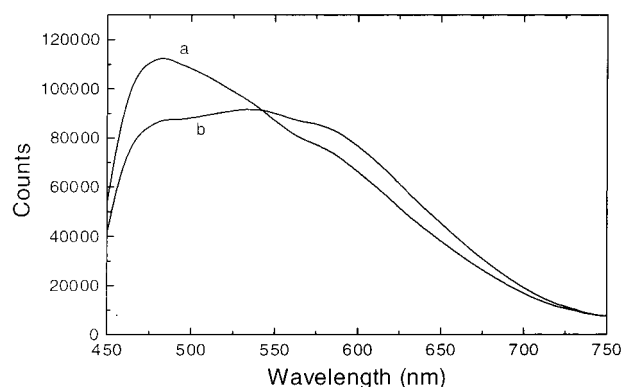


Figure 4. Room-temperature emission spectra of the TPY (a) and $(\text{TP}^+/\text{TiO}_2)\text{-Y}$ (b) samples upon 420 nm excitation. The area of the photoluminescence spectra from 540 to 700 nm was $(8.6 \pm 0.1) \times 10^6$ and $(7.4 \pm 0.2) \times 10^6$ for a and b, respectively.

TABLE 1: Analytical and Spectroscopic Data for the Samples Prepared in This Work

sample	photosensitizer/ Ti loading ^a	λ_{max}^b (nm)	$\bar{\nu}^c$ (cm^{-1})
$\text{Ru}(\text{bpy})_3^{2+}\text{-Y}$	1 $\text{Ru}(\text{bpy})_3^{2+}$ in 6 supercages	440	1422
		456	1467
			1525
$(\text{Ru}(\text{bpy})_3^{2+}/\text{TiO}_2)\text{-Y}$	> 4.7 Ti atoms/ supercage	250	1693
		440	
		456	
TPY	1 TP^+ in 3 supercages	366	1620, 1595
		410	1579, 1494
			1471, 1448
$(\text{TP}^+/\text{TiO}_2)\text{-Y}$	3.8 Ti atoms/ supercage	250	1693
		366	
		410	

^a From C, N, and Ti elemental analyses. ^b From diffuse reflectance UV–vis spectra. ^c From the IR spectra of self-supported wafers after outgassing at 200 °C under 10^{-2} Pa for 1 h.

corresponds closely to the fluorescence, up to a 20% decrease in intensity was observed.

We performed time-resolved fluorescence studies to determine whether the decrease in total emission is due to a dynamic and/or a static quenching process. The occurrence of dynamic quenching, i.e., an interaction developing during the lifetime of the excited probe, due to the interaction between the photosensitizers and TiO_2 , should be reflected in the emission decay kinetics as well as in the overall emission intensity. Considering that all components in the systems under investigation are immobile within the lifetime of the excited state,

TABLE 2: Fluorescence Decay Kinetic Parameters Determined for the Samples Studied

sample	k_1	A_1	k_2	A_2	k_3 (ns ⁻¹)	A_3	k_{av}^a
Ru(bpy) ₃ ²⁺ -Y	2.73 μs ⁻¹	0.42	1.14 μs ⁻¹	0.56			1.79 μs ⁻¹
(Ru(bpy) ₃ ²⁺ /TiO ₂)-Y	2.31 μs ⁻¹	0.47	1.05 μs ⁻¹	0.56			1.67 μs ⁻¹
TPY	3.00 ns ⁻¹	0.74	0.70 ns ⁻¹	0.23	0.16	0.04	2.39 ns ⁻¹
(TP ⁺ /TiO ₂)-Y (0.2 M)	3.26 ns ⁻¹	0.92	0.70 ns ⁻¹	0.21	0.16	0.03	3.15 ns ⁻¹
(TP ⁺ /TiO ₂)-Y (0.4 M)	3.22 ns ⁻¹	1.02	0.75 ns ⁻¹	0.15	0.16	0.01	3.40 ns ⁻¹

^a These values are obtained from the average of the decay rate constants weighed by their preexponential values.

emission quenching should be static in essence. In the case of samples containing TP⁺ emission quenching was investigated using a picosecond time-resolved fluorescence setup. Analysis of the obtained traces (see Table 2 and Figure 5B) shows that the decays are best fitted by a triexponential expression in these systems. We cannot rule out some phosphorescence contribution, which together with background noise would account for variations in the lifetimes observed in each of the three samples studied, i.e., TPY and TP/TiO₂-Y prepared with two different loadings of TiO₂. From the weight of the rate constants, as indicated by their preexponential factors, we conclude that the contribution of the smaller rate constant is negligible, particularly at higher loading of TiO₂. It is also clear from Table 2 that for the three samples studied the weight of the faster component increases with increasing TiO₂ content. However, the instrument response, ca. 100 ps, does not enable a clear differentiation of fast events, and the observed fast component could be, in reality, the result of more than one process. This prompts us to conclude that the observed reduction in the total fluorescence, as observed in steady-state experiments, is due to a decrease in the amount of dye presenting a longer decay component. This results from quenching of the dye by TiO₂ within 100 ps or less and, therefore, cannot be resolved from the fast component of the TP⁺ decay; for practical purposes, what we observe is static quenching.

In view of the long lifetime of Ru(bpy)₃²⁺-Y samples, ca. 1 μs, their analysis was best accomplished using nanosecond laser excitation. No change in lifetime (see Table 2 and Figure 5A) was observed when comparing the emission of samples before and after incorporation of TiO₂. This clearly indicates that no dynamic quenching is taking place in these systems. Previous work on the photoluminescence quenching of Ru(bpy)₃²⁺ excited states by methyl viologen incorporated within zeolites has established that the occurrence of static⁴¹ or dynamic⁴⁵ processes is dependent on the extra- or intrazeolitic location of Ru(bpy)₃²⁺. The dynamic component was interpreted as due to the diffusion of small methyl viologen molecules that are able to interact with excited Ru(bpy)₃²⁺ within its relatively long lifetime. Results showing the absence of a significant dynamic component for the quenching of TP⁺ or Ru(bpy)₃²⁺ by TiO₂ within zeolite Y are consistent with the expected lack of diffusion of the dye and TiO₂ clusters through the zeolite micropores. As a consequence, only those excited photosensitizer molecules in direct contact with TiO₂ clusters are quenched. An analogous conclusion was reached in a recent report on Ru(bpy)₃²⁺-TiO₂ systems in zeolite Y.⁶¹

The results indicate that static quenching is operating for both photosensitizers; i.e., quenching occurs "instantaneously", within the time resolution of our instrumentation, after dye excitation and results in a nonemissive relaxation of the species by interaction with the quencher. While this static quenching could have been anticipated on the basis of the well-known fast interfacial electron injection interaction between related Ru(bpy)₃²⁺ complexes bound to the surface of TiO₂ particles, the interaction of an electron-accepting dye such as TP⁺ is unprecedented and presumably should occur through a mech-

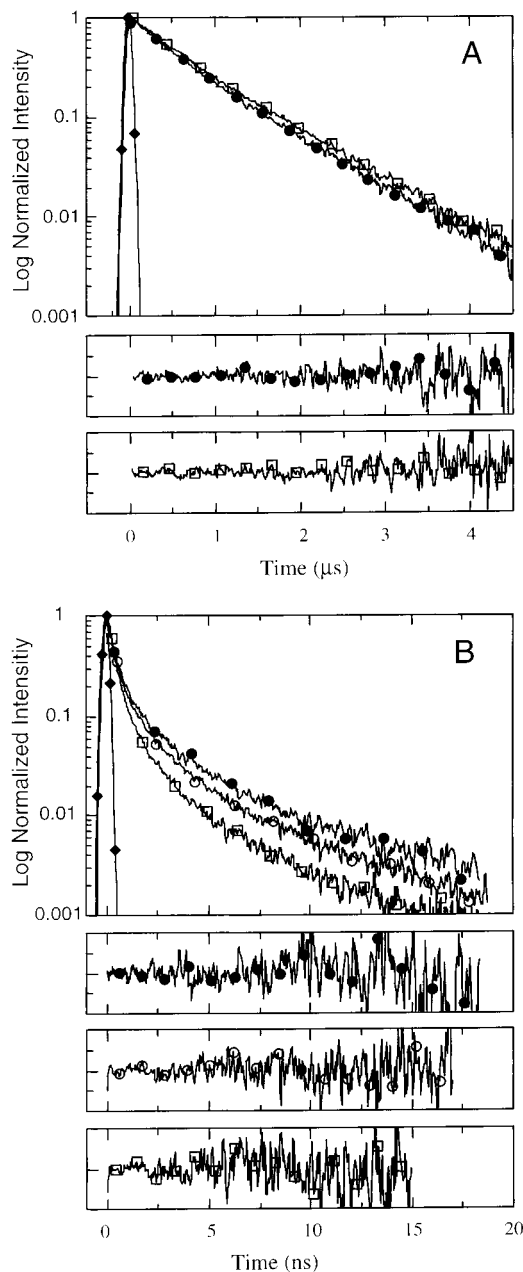


Figure 5. (A) Fluorescence decay of Ru(bpy)₃²⁺ alone in zeolite Y (●) and co-included with TiO₂ in zeolite Y (□) following 355 nm irradiation with a 6 ns laser pulse (◆) under N₂ atmosphere. (B) Fluorescence decay of TP alone in zeolite Y (●) and co-included with TiO₂ in zeolite Y (prepared in 0.2 M (○) and 0.4 M (□) aqueous solutions containing (NH₄)₂(Ti=O)(C₂O₄)₂·H₂O) following 355 nm irradiation with a 100 ps laser pulse (◆) under N₂ atmosphere. Also shown are the residuals for the fitting; the fitting curve parameters are presented in Table 2.

anism opposite from that of Ru(bpy)₃²⁺, i.e., electron abstraction from the valence band and generation of positive holes in the TiO₂ semiconductor.

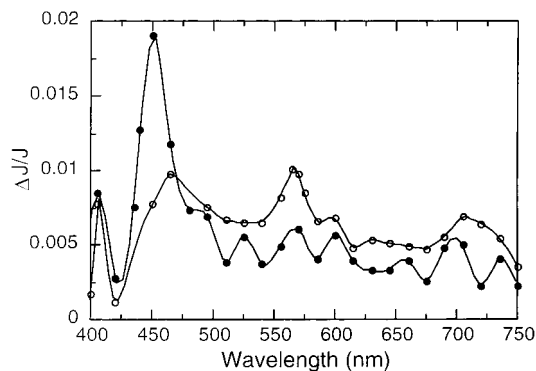


Figure 6. Transient diffuse reflectance spectra recorded $\sim 6 \mu\text{s}$ after 355 nm laser excitation for samples of zeolite Y containing only TP^+ cation (\bullet) or both TP^+ and TiO_2 (\circ). The TP^+ triplet is seen at 450 nm, and the TP^* radical at 570 nm.

To further understand the nature of the quenching between excited TP^+ and TiO_2 , time-resolved DRS studies were carried out using nanosecond laser flash photolysis. In a previous work we have established that, in the absence of any quencher, laser flash photolysis of TP^+ encapsulated within zeolite Y leads to the generation of the triplet excited state that decays with a lifetime of hundreds of microseconds.⁶⁴ This is the behavior observed for the original TPY sample prior to the incorporation of TiO_2 upon 308 or 355 nm excitation (Figure 6). However, after the incorporation of TiO_2 in the solid, the transient DRS spectrum is clearly different from that of the original TPY samples. In addition to the presence of residual TP^+ triplet excited state, generation of TP^* radical characterized by a well-defined absorption peak at 570 nm^{65,66} is also observed (Figure 6). The lifetime of the residual triplet excited-state remains identical to that of the TPY samples not containing TiO_2 , approximately 55% of triplet states are quenched in the presence of TiO_2 . This is consistent with the lack of dynamic quenching in the emission of these samples. These observations indicate that the triplet excited states monitored by laser flash photolysis do not interact with TiO_2 within their lifetime due to the lack of diffusion together of probe and quencher, as has been similarly observed for the singlet excited state. One consequence of singlet state static quenching may be that triplets are generated only at framework locations where the excited molecules are spatially separated from TiO_2 clusters. Those excited TP^+ ions in intimate contact with TiO_2 undergo an electron transfer from the electron donor to excited TP^+ , leading to the formation of the observed TP^* pyryl radical. This is a static quenching process, since the growth of the signal for TP^* (λ_{max} 570 nm) is not observed within the nanosecond time scale available to our setup. On the basis that the main difference between TPY and $(\text{TP}^+/\text{TiO}_2)\text{-Y}$ is the presence of TiO_2 clusters, it is reasonable to assign the role of electron donor to the TiO_2 . This behavior is exactly the reverse of the well-established electron injection observed for the $\text{Ru}(\text{bpy})_3^{2+}/\text{TiO}_2$ couple. Electrochemical measurements using zeolite-modified electrodes gives for the reduction potential of TP^+ encapsulated within the interior of zeolite Y a value of -0.28 V vs SCE in acetonitrile. That is the same value is that measured for other soluble TP^+ salts in solution. By use of the energy of the singlet excited state for encapsulated TP^+ estimated from the absorption and emission spectra as 65 kcal/mol and by application of the Rehm–Weller equation, it is calculated that TP^+ encapsulated inside the pores of zeolite Y has an oxidation potential of about 2.5 V, which is a comparatively very high oxidation potential. In fact electrochemical measurements for a modified zeolite electrode of a $\text{TiO}_2@\text{Y}$ sample (without containing TP^+) yield an oxidation

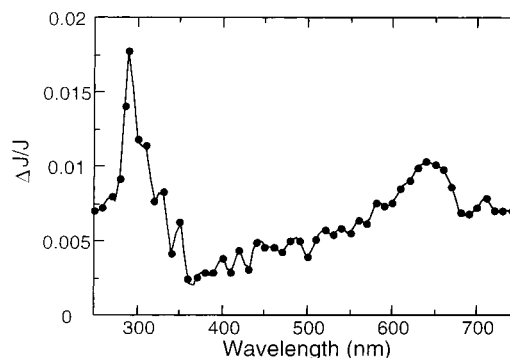


Figure 7. Transient diffuse reflectance spectrum generated from $\text{Ru}(\text{bpy})_3^{2+}$ co-included with TiO_2 in zeolite Y. The spectrum was recorded under nitrogen $6.4 \mu\text{s}$ after the 532 nm laser pulse.

potential of 1.2 V vs SCE for TiO_2 clusters, which clearly establishes the thermodynamic feasibility of the proposed oxidation.

As anticipated, on the basis of the information for related $\text{Ru}(\text{bpy})_3^{2+}/\text{TiO}_2$ systems, 532 nm laser excitation gives rise to the generation of $\text{Ru}(\text{bpy})_3^{3+}$ as a long-lived transient characterized by a sharp ligand-centered absorption band at $\sim 300 \text{ nm}$ and a broad metal-to-ligand charge-transfer band at 650 nm (Figure 7).

The relative photocatalytic efficiencies of these two-component systems were compared with those for analogous samples containing only one of the components and also with commercial TiO_2 anatase. As a test reaction, we selected the photodeactivation of the enzymatic activity of horseradish peroxidase.

The photocatalytic activity of TiO_2 has been studied in relationship with biologically relevant substrates in aqueous solution.^{67–75} Studies with amino acids and nucleic acids have shown that irradiation with UVA light in the presence of TiO_2 catalyzes the degradation of these biomolecules.

An earlier study by our group has shown that TiO_2 particles in aqueous suspension efficiently deactivate horseradish peroxidase (HRP),⁷⁶ an enzyme that decomposes H_2O_2 in the presence of a suitable substrate. HRP belongs to a large family of peroxidases widely distributed in nature. Photoinduced deactivation of HRP by TiO_2 occurs both under anaerobic and aerobic conditions, but it is far more effective in the latter case. The process occurs concurrently with the destruction of the heme group, which is the catalytic center in these enzymes. It is likely that while damage is most pronounced at the heme group, reactions also occur at the protein frame.

We have thus studied the photocatalytic behavior of the two-component TP^+/TiO_2 or $\text{Ru}(\text{bpy})_3^{2+}/\text{TiO}_2$ photocatalytic systems included in zeolite Y in an aqueous buffered media containing HRP as a biological substrate and made comparisons with the behavior of the isolated components TP^+ , $\text{Ru}(\text{bpy})_3^{2+}$, or TiO_2 included in zeolite Y and bulk TiO_2 anatase. Irradiation of the solutions was performed at 350 nm to avoid direct absorption of light by the protein. Following the irradiation, the activity of HRP was assayed in the presence of 2,2'-azinobis(3-ethylbenzthiazoline-6-sulfonic acid) diammonium salt (ABTS) as a substrate. Control experiments were done with samples irradiated without the different catalysts as well as with nonirradiated samples in the presence of these catalysts.

The results are shown in Figure 8. Those zeolite photocatalysts simultaneously incorporating the photosensitizer and nanoscopic TiO_2 clusters as relay are more active than those containing only one of the components. The series of TP^+ -based

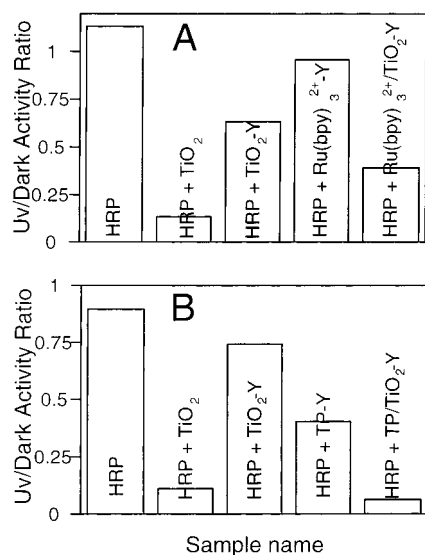
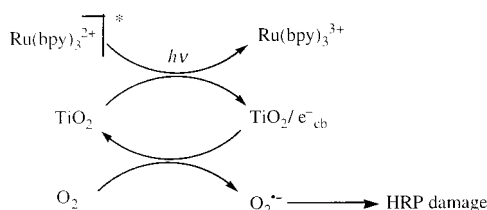
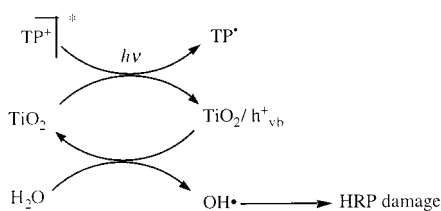


Figure 8. Relative enzymatic activity measured for HRP in water and in the presence of different photocatalysts as indicated. A: Ru(bpy)₃²⁺ photocatalysts; B: TP⁺ photocatalysts. Results are the average of three measurements. Activity values were obtained from the coefficient *b* of the fitting curve for each sample. Dark samples exhibited an activity value of 0.15 units of absorbance change at 412 nm s⁻¹/(4 ng/mL of enzyme). With these values the ratio of activities for light exposed and unexposed samples was determined.

SCHEME 3



SCHEME 4



photocatalysts are more active than those of Ru(bpy)₃²⁺. As a working hypothesis, this trend can be explained as indicating that reactive oxygen species derived from OH• (generated by electron abstraction from water by h⁺ of the TiO₂ relay, in the case of TP⁺) produce more HRP deactivation than those arising from O₂^{•-} (generated by electron injection from the conduction band of TiO₂ to molecular oxygen, in the case of Ru(bpy)₃²⁺), as shown in Schemes 3 and 4. The case of TP⁺/TiO₂-Y is remarkable, since the synergism between the two components is unequivocal. The photocatalytic activity of (TP⁺/TiO₂)-Y even overcomes that of pure anatase under the conditions studied. To support the intermediary of OH•, a TiO₂@Y sample was irradiated through quartz, wherein a stationary concentration of 10⁻³ M H₂O₂ (the coupling product of two OH• radicals) was measured.

In summary, time-resolved emission and absorption spectroscopy show unambiguously that the photochemical properties of encapsulated dyes are modified by the presence of codoped TiO₂ nanoclusters. The organized and compartmentalized space

of the zeolite micropores holds in place and allows intimate contact between the electron donor or acceptor photosensitizer and the nanoscopic TiO₂ relay without the need for covalent bonding. This interaction is essentially instantaneous in the nanosecond time scale, and only static quenching processes can be observed with a residual population of excited dyes remaining unaffected by the presence of codoped TiO₂ clusters. Photoactivation of HRP, as a test reaction in aqueous medium, clearly establishes that the photocatalytic activity of zeolites containing the photosensitizing dye/TiO₂ combination exhibits a synergism when compared to that for the isolated components encapsulated in zeolite Y, confirming the role of TiO₂ as an efficient electron or hole relay.

Experimental Section

TPY was prepared by reacting a suspension of 2 equiv of chalcone and acetophenone in isooctane in the presence of thermally dehydrated HY (Si/Al = 2.4) at 110 °C for 7 days, as reported.¹⁸ The sample of Ru(bpy)₃²⁺-Y was obtained by ion exchange of a commercial NaY sample (Aldrich LYZ-53) with a diluted [Ru(NH₃)₆]Cl₃ aqueous solution followed by addition of an excess of bipyridine and exhaustive solid-liquid extraction for 2 weeks according to the method originally reported by Herron.^{77,78} The samples containing TiO₂ were prepared by stirring suspensions of the required zeolite for 1 h at room temperature in aqueous solutions containing 0.1 or 0.4 M (NH₄)₂(Ti=O)(C₂O₄)₂·H₂O. This was followed by mild calcination at 150 °C according to a literature procedure.²³

FT-IR spectra were obtained using a Nicolet 710 FT spectrophotometer. Self-supported zeolite wafers (~10 mg) were compressed at 1 ton·cm⁻² for 3 min and placed in sealed greaseless cells with CaF₂ windows. The cells were outgassed at 200 °C under 10⁻² Pa for 1 h before recording the spectrum at room temperature. DRS were recorded with a Cary 5G spectrophotometer using a praying mantis attachment and BaSO₄ as a standard. To correct direct scattering, the absorption of the samples was obtained from the diffuse reflectance of each sample subtracting that of the pristine zeolite Y. Steady-state emission spectra were recorded at room temperature in an Edinburgh FL900 spectrofluorometer using the reported absorption wavelength maxima for excitation. The powder zeolite samples were placed in septum-capped Suprasil quartz cells and purged with nitrogen for at least 15 min prior to recording the emission. The spectra shown in Figures 3 and 4 correspond to the average of 18 independent measurements of the emission of samples with and without TiO₂. Recording of the emission spectra was done in random order, on different days, placing each time fresh powder in the cell.

Time-resolved DRS measurements were made using the second (532 nm) or third (355 nm) harmonic pulse from a Surelite Nd:YAG laser (≤10 ns pulse width; ≤20 mJ pulse⁻¹) or a Lumonics EX-530 excimer laser (308 nm; ≤10 ns pulse width; ≤100 mJ pulse⁻¹) as excitation sources. Signals from the photomultiplier tube were captured and digitized by a Tektronix 24 transient digitizer and transferred to a Power Macintosh programmed in the LabView environment. Details of similar time-resolved diffuse reflectance systems have been described elsewhere.⁷⁹⁻⁸¹ Samples were irradiated in 3 × 7 mm² Suprasil quartz cells and were purged with nitrogen for at least 30 min prior to each experiment.

Time-resolved photoluminescence studies were carried out using the second (532 nm) or third (355 nm) harmonic pulse from a Continuum PY-61 Nd:YAG laser (35 ps, 4 mJ pulse⁻¹)

as the excitation source. A Hamamatsu C4334 streak camera was used for time-resolved fluorescence detection and data acquisition.⁸² The instrument time resolution is ca. 100 ps. Samples were irradiated in 3×7 mm² Suprasil quartz cells and were purged with nitrogen for at least 30 min prior to each experiment.

Horseradish Peroxidase Inactivation. The titanium dioxide pure anatase sample, used as control, with an average particle size of 32 nm, was purchased from Alfa Aesar. Horseradish peroxidase (HRP), type VI-A, and 2,2'-azinobis(3-ethylbenz-thiazoline-6-sulfonic acid) diammonium salt (ABTS) were purchased from Sigma and used as received. All buffers were prepared using filtered Millipore water (Millipore Milli-Q system) and reagent grade chemicals. All buffers were treated with a chelating resin, iminodiacetic acid from Sigma, to remove any traces of metal ions.

TPY, Ru(bpy)₃²⁺-Y (and their TiO₂ loaded counterparts), TiO₂-Y and TiO₂ anatase suspensions, and HRP solutions were prepared also in Millipore water.

Steady-state photolyses were performed using an irradiation chamber fitted with 350 nm Luzchem UVA lamps. Samples containing only HRP (0.1 mg mL⁻¹) as well as those containing both enzyme and loaded zeolite (1.0 mg mL⁻¹) or enzyme and TiO₂ anatase (0.1 mg mL⁻¹) were photolyzed in Pyrex test tubes (1 cm i.d., 5 mL total volume). Dark control samples were placed in the chamber to ensure all samples (exposed and unexposed) had the same history. HRP activity assays were performed with [ABTS] = 0.025 mM and [H₂O₂] = 0.25 mM, prepared in a buffer of pH 4.4; this choice of pH was dictated by the assay procedure. To 5 mL of the solution of ABTS and H₂O₂ was added a diluted fraction, ~20 ng, of the enzyme (HRP solutions were diluted 1/4500 for the assay) according to the assay procedure of Porstmann et al.⁸³ All activity assays were monitored at 412 nm using a Milton-Roy 3000 UV-visible spectrophotometer in kinetics mode. Absorption spectra were acquired on the same instrument used in scan mode. Plots of kinetic data were constructed using Kaleidagraph software and fitted with a second-order polynomial equation to determine the initial slopes. Each curve is then fitted with the expression⁷⁶

$$A_{412\text{ nm}} = a + bt + ct^2$$

where A is the absorbance and t the time. The coefficients a – c are fitting parameters. The derivative of this expression with respect to t is given by

$$\frac{dA_{412\text{ nm}}}{dt} = b + 2ct$$

which at $t = 0$ corresponds to b . That is, the first coefficient (b) of the quadratic fit is the calculated initial slope. These slopes have been used as a measure of the enzymatic activity.

Acknowledgment. Financial support by the Spanish DGI-CYT (H.G., Grant MAT2000-1768-CO2-01) and NSERC (Canada) through operating and strategic grants (J.C.S.) is gratefully acknowledged. H.G. thanks the Spanish DGES for a fellowship at the University of Ottawa (Grant PR2000-0040).

References and Notes

- (1) *Photochemistry in Organized and Constrained Media*; Ramamurthy, V., Ed.; VCH: New York, 1991.
- (2) Persaud, L.; Bard, A. J.; Champion, A.; Fox, M. A.; Mallouk, T. E.; Webber, S. E.; White, J. M. *J. Am. Chem. Soc.* **1987**, *109*, 7309.

- (3) Yonemoto, E. H.; Kim, Y. I.; Schmechl, R. H.; Wallin, J. O.; Shoulders, B. A.; Richardson, B. R.; Haw, J. F.; Mallouk, T. E. *J. Am. Chem. Soc.* **1994**, *116*, 10557.
- (4) Kim, Y. I.; Keller, S. W.; Krueger, J. S.; Yonemoto, E. H.; Saupe, G. B.; Mallouk, T. E. *J. Phys. Chem. B* **1997**, *101*, 2491.
- (5) Sykora, M.; Maruszewski, K.; Treffet, Z.; Shelly, M.; Kincaid, J. R. *J. Am. Chem. Soc.* **1998**, *120*, 3490.
- (6) Haag, W. O.; Lago, R. M.; Weisz, *Nature* **1984**, *309*, 589.
- (7) Wright, P. A.; Thomas, J. M.; Cheetham, A. K.; Novak, A. K. *Nature* **1985**, *318*, 611.
- (8) Derouane, E. G. *J. Catal.* **1986**, *100*, 541.
- (9) Parton, F. R.; Vankelecom, I. F. J.; Casselman, M. J. A.; Bezoukhanova, C. P.; Uytterhoeven, J. B.; Jacobs, P. A. *Nature* **1994**, *370*, 541.
- (10) Thomas, J. M. *Angew. Chem., Int. Ed. Engl.* **1994**, *33*, 913.
- (11) Raja, R.; Ratnasamy, P. *J. Mol. Catal.* **1995**, *1995*, 93.
- (12) Scaiano, J. C.; García, H. *Acc. Chem. Res.* **1999**, *32*, 783.
- (13) Sankararaman, S.; Yoon, K. B.; Yabe, T.; Kochi, J. K. *J. Am. Chem. Soc.* **1991**, *113*, 1419.
- (14) Scaiano, J. C.; Camara de Lucas, N.; Andraos, J.; García, H. *Chem. Phys. Lett.* **1995**, *233*, 5.
- (15) Gfeller, N.; Calzaferri, G. *J. Phys. Chem. B* **1997**, *101*, 1396.
- (16) Gfeller, N.; Megelski, S.; Calzaferri, G. *J. Phys. Chem. B* **1999**, *103*, 1250.
- (17) Ramamurthy, V.; Lakshminarasimhan, P.; Grey, P. C.; Johnston, L. *Chem. Commun.* **1998**, 2411.
- (18) Corma, A.; Fornés, V.; García, H.; Miranda, M. A.; Primo, J.; Sabater, M. J. *J. Am. Chem. Soc.* **1994**, *116*, 2276.
- (19) Fornés, V.; García, H.; Miranda, M. A.; Mojarrad, F.; Sabater, M.-J.; Suliman, N. N. E. *Tetrahedron* **1996**, *52*, 7755.
- (20) Sanjuán, A.; Aguirre, G.; Alvaro, M.; García, H. *Appl. Catal., B* **1998**, *15*, 247.
- (21) Sanjuán, A.; Alvaro, M.; Corma, A.; García, H. *Chem. Commun.* **1999**, 1641.
- (22) Sanjuán, A.; Aguirre, G.; Alvaro, M.; García, H.; Scaiano, J. C. *Appl. Catal., B* **2000**, *25*, 257.
- (23) Liu, X.; Iu, K.-K.; Thomas, J. K. *J. Chem. Soc., Faraday Trans.* **1993**, *89*, 1861.
- (24) Fox, M. A.; Doan, K. E.; Dulay, M. T. *Res. Chem. Intermed.* **1994**, *20*, 711.
- (25) Yamashita, H.; Ichihashi, Y.; Anpo, M.; Hashimoto, M.; Louis, C.; Che, M. *J. Phys. Chem.* **1996**, *100*, 16041.
- (26) Yamashita, H.; Honda, M.; Harada, M.; Ichihashi, Y.; Anpo, M.; Hirao, T.; Itoh, N.; Iwamoto, N. *J. Phys. Chem. B* **1998**, *102*, 10707.
- (27) Yamashita, H.; Fujii, Y.; Ichihashi, Y.; Zhang, S. G.; Ikeue, K.; Park, D. R.; Koyano, K.; Tatsumi, T.; Anpo, M. *Catal. Today* **1998**, *45*, 221.
- (28) Klass, J.; Schulz-Ekloff, G.; Jaeger, N. I. *J. Phys. Chem. B* **1997**, *101*, 1305.
- (29) Grubert, G.; Wark, M.; Jaeger, N. I.; Schulz-Ekloff, G. *J. Phys. Chem. B* **1998**, *102*, 1665.
- (30) Xu, Y.; Langford, C. H. *J. Phys. Chem.* **1995**, *99*, 11501.
- (31) Xu, Y.; Langford, C. H. *J. Phys. Chem. B* **1997**, *101*, 3115.
- (32) Anpo, M.; Yamashita, H.; Ichihashi, Y.; Fujii, Y.; Honda, M. *J. Phys. Chem. B* **1997**, *101*, 2632.
- (33) Anpo, M.; Yamashita, H.; Matsuoaka, M.; Park, D. R.; Shul, Y. G.; Park, S. E. *J. Ind. Eng. Chem.* **2000**, *6*, 59.
- (34) Corrent, S.; Cosa, G.; Scaiano, J. C.; Galletero, M. S.; Alvaro, M.; García, H. *Chem. Mater.* **2001**, *13*, 715.
- (35) Cosa, G.; Galletero, M. S.; Fernández, L.; Márquez, F.; García, H.; Scaiano, J. C. Submitted for publication.
- (36) Miranda, M. A.; García, H. *Chem. Rev.* **1994**, *94*, 1063.
- (37) Borja, M.; Dutta, P. K. *Nature* **1993**, *362*, 43.
- (38) Krueger, J. S.; Mayer, J. E.; Mallouk, T. E. *J. Am. Chem. Soc.* **1988**, *110*, 8232.
- (39) Yonemoto, E. H.; Kim, Y. I.; Schmechl, R. H.; Wallin, J. O.; Shoulders, B. A.; Richardson, B. R.; Haw, J. F.; Mallouk, T. E. *J. Am. Chem. Soc.* **1994**, *116*, 10557.
- (40) Dutta, P. K.; Turbeville, W. J. *J. Phys. Chem.* **1992**, *96*, 9410.
- (41) Turbeville, W.; Robins, D. S.; Dutta, P. K. *J. Phys. Chem.* **1992**, *96*, 5024.
- (42) Dutta, P. K.; Incavo, J. A. *J. Phys. Chem.* **1987**, *91*, 4443.
- (43) Villemure, G.; Pinnavaia, T. J. *Chem. Mater.* **1999**, *11*, 789.
- (44) Brigham, E. S.; Snowden, P. T.; Kim, Y. I.; Mallouk, T. E. *J. Phys. Chem.* **1993**, *97*, 8650.
- (45) Kim, Y. I.; Mallouk, T. E. *J. Phys. Chem.* **1992**, *96*, 2879.
- (46) Sykora, M.; Kincaid, J. R.; Dutta, P. K.; Castagnola, N. B. *J. Phys. Chem. B* **1999**, *103*, 309.
- (47) DeWilde, W.; Peeters, G.; Lunsford, J. H. *J. Phys. Chem.* **1980**, *84*, 2306.
- (48) Qualey, W. H.; Lunsford, J. H. *Inorg. Chem.* **1982**, *21*, 97.
- (49) Lunsford, J. *J. ACS Symp. Ser.* **1977**, *40*, 473.
- (50) O'Regan, B.; Grätzel, M. *Nature* **1991**, *335*, 737.

- (51) Nazeeruddin, M. K.; Kay, A.; Rodicio, I.; Humphry-Baker, R.; Müller, E.; Liska, P.; Vlachopoulos, N.; Grätzel, M. *J. Am. Chem. Soc.* **1993**, *115*, 6382.
- (52) Nazeeruddin, M. K.; Péchy, P.; Grätzel, M. *Chem. Commun.* **1997**, 1705.
- (53) Amadelli, R.; Argazzi, R.; Bignozzi, C. A.; Scandola, F. *J. Am. Chem. Soc.* **1990**, *112*, 7029.
- (54) Alebbi, M.; Bignozzi, C. A.; Heimer, T. A.; Hasselmann, G.; Meyer, G. *J. Phys. Chem. B* **1998**, *102*, 7577.
- (55) Islam, A.; Sugihara, H.; Hara, K.; Singh, L. P.; Katoh, R.; Yanagida, M.; Takahashi, Y.; Murata, S.; Arakawa, H. *New J. Chem.* **2000**, *24*, 343.
- (56) Park, N.-G.; Schlichthörl, G.; van de Lagemaat, J.; Cheong, H. M.; Mascarenhas, A.; Frank, A. J. *J. Phys. Chem. B* **1999**, *103*, 3308.
- (57) Hagfeldt, A.; Grätzel, M. *Acc. Chem. Res.* **2000**, *33*, 269.
- (58) Cahen, D.; Hodes, G.; Grätzel, M.; Guillemoles, J. F.; Riess, I. *J. Phys. Chem. B* **2000**, *104*, 2053.
- (59) He, J.; Zhao, J.; Shen, T.; Hidaka, H.; Serpone, N. *J. Phys. Chem. B* **1997**, *101*, 9027.
- (60) Tachibana, Y.; Haque, S. A.; Mercer, I. P.; Durrant, J. R.; Klug, D. R. *J. Phys. Chem. B* **2000**, *104*, 1198.
- (61) Bossmann, S. H.; Turro, C.; Schnabel, C.; Pokhrel, M. R.; Payawan, L. M., Jr.; Baumeister, J. B.; Wörner, M. *J. Phys. Chem. B* **2001**, *105*, 5374.
- (62) Liu, X.; Iu, K. K.; Thomas, J. K. *Chem. Phys. Lett.* **1992**, *195*, 163.
- (63) Wintgens, V.; Kossanyi, J.; Simalty, M. *Bull. Soc. Chim. Fr.* **2** **1983**, 115.
- (64) Cano, M. L.; Cozens, F. L.; García, H.; Martí, V.; Scaiano, J. C. *J. Phys. Chem.* **1996**, *100*, 18152.
- (65) Niizuma, S.; Sato, N.; Kawata, H.; Suzuki, I.; Toda, T.; Kokubun, H. *Bull. Chem. Soc. Jpn.* **1985**, *58*, 2600.
- (66) Wintgens, V.; Pouliquen, J.; Kossany, J.; Heinz, M. *Nouv. J. Chim.* **1986**, *10*, 345.
- (67) Dhananjeyan, M. R.; Annapoorani, R.; Renganathan, R. *J. Photochem. Photobiol., A* **1997**, *109*, 147.
- (68) Dunford, R.; Salinaro, A.; Cai, L. Z.; Serpone, N.; Horikoshi, S.; Hidaka, H.; Knowland, J. *Febs Lett.* **1997**, *418*, 87.
- (69) Hidaka, H.; Horikoshi, S.; Ajisaka, K.; Zhao, J.; Serpone, N. *J. Photochem. Photobiol., A* **1997**, *108*, 197.
- (70) Hidaka, H.; Shimura, T.; Ajisaka, K.; Horikoshi, S.; Zhao, J. C.; Serpone, N. *J. Photochem. Photobiol., A* **1997**, *109*, 165.
- (71) Hidaka, H.; Horikoshi, S.; Serpone, N.; Knowland, J. *J. Photochem. Photobiol., A* **1998**, *111*, 205.
- (72) Hidaka, H.; Ajisaka, K.; Horikoshi, S.; Oyama, T.; Zhao, J. C.; Serpone, N. *Catal. Lett.* **1999**, *60*, 95.
- (73) Horikoshi, S.; Serpone, N.; Zhao, J. C.; Hidaka, H. *J. Photochem. Photobiol., A* **1998**, *118*, 123.
- (74) Horikoshi, S.; Serpone, N.; Yoshizawa, S.; Knowland, J.; Hidaka, H. *J. Photochem. Photobiol., A* **1999**, *120*, 63.
- (75) Wamer, W. G.; Yin, J. J.; Wei, R. R. *Free Radical Biol. Med.* **1997**, *23*, 851.
- (76) Hancock-Chen, T.; Scaiano, J. *J. Photochem. Photobiol., B* **2000**, *57*, 193.
- (77) Herron, N.; Stucky, G. D.; Tolman, C. A. *J. Chem. Soc., Chem. Commun.* **1986**, 1521.
- (78) Herron, N. *Inorg. Chem.* **1986**, *25*, 4714.
- (79) Wilkinson, F.; Willsher, C. *J. Appl. Spectrosc.* **1984**, *38*, 897.
- (80) Scaiano, J. C.; Tanner, M.; Weir, D. *J. Am. Chem. Soc.* **1985**, *107*, 4396.
- (81) Wilkinson, F.; Kelly, G. Diffuse Reflectance Flash Photolysis. In *Handbook of Organic Photochemistry*; Scaiano, J. C., Ed.; CRC Press: Boca Raton, FL, 1989; Vol. 1; p 293.
- (82) Mohtat, N.; Cozens, F. L.; Scaiano, J. C. *J. Phys. Chem. B* **1998**, *102*, 7557.
- (83) Porstmann, B.; Porstmann, T.; Nugel, M. *J. Clin. Chem. Biochem.* **1981**, *19*, 435.